SYNTHESIS OF Fe_3O_4 NANOPARTICLES GROWN ON RICE HUSK WASTE-DERIVED POROUS CARBON FOR HIGH-EFFICIENCY MICROWAVE ABSORPTION

Van Thin Pham[1], Dinh Vi Le[1], Van Tuan Nguyen[1], Tran Ha Nguyen[1], Vu Tung Nguyen[1], Thi Thanh Nguyen[1], Quang Dat Tran[1,*]

[1]*Faculty of Physics and Chemical Engineering, Le Quy Don Technical University, Hanoi, Vietnam*

Abstract

In this study, a straightforward process was employed to synthesize Fe_3O_4 nanoparticles-decorated porous carbon derived from rice husk waste (Fe_3O_4/C). The composite material was made by using pyrolysis and then coprecipitation. Fe_3O_4 nanoparticles were dispersed evenly across the surface of a porous carbon structure made from rice husks (PC) in three dimensions (3D). The highly graphitized porous carbon framework makes the tracks for electromagnetic waves that propagate longer and increases the loss of conductivity. With its unique structure and the effects of great attenuation and good impedance matching, Fe_3O_4/C is much better at absorbing microwaves than pure porous carbon. Most samples have a minimum reflection loss (RL) of less than -10 dB (90% reduction) over a wide range of electromagnetic frequencies (3.6 - 18.0 GHz) when the thickness of the absorber varies from 1.5 - 4.0 mm. With a thickness of 3.0 mm, the best RL is -70.8 dB, and with a thin thickness of 1.5 mm, the effective absorption bandwidth (EAB) is 14.4 GHz. According to the findings of this study, the use of Fe_3O_4/C material for electromagnetic wave absorption applications holds great promise due to the low cost and extensive benefits of the preparation process, as well as its excellent electromagnetic absorption performance.

Keywords*: Fe_3O_4; ferrite; biomass; rice husk; microwave absorber.*

1. Introduction

The exponential growth of telecommunication gadgets has brought forth unparalleled prospects for societal advancement and addressing public demands [1]. Nevertheless, this sudden increase unavoidably gives rise to a multitude of electromagnetic (EM) difficulties, including concerns such as electromagnetic interference (EMI), electromagnetic pollution, and electromagnetic leakage [2]. The increasing need to address the issue of severe electromagnetic pollution has prompted a pressing search for improved materials capable of absorbing microwaves. The utilization of microwave absorption presents an innovative approach to tackle these difficulties, by

* Email: dattq@lqdtu.edu.vn
DOI: 10.56651/lqdtu.jst.v1.n02.692.pce

directing EM energy towards thermal or other energy sources, resulting in the creation of an ideal EM environment [3].

Carbon compounds are notable in the realm of dielectric loss materials because of their impressive conductivity and the presence of many functional groups on their surfaces, which act as polarized centers. The distinctive features of these phenomena have sparked significant research interest in the field of electromagnetic absorption [4]. Porous carbon composites, which are derived from biomass, demonstrate notable characteristics in terms of their lightweight nature and effectiveness in microwave absorption [5]. With a minimum reflection loss (RL_{min}) of -47.5 dB at 2.8 mm and an effective absorption bandwidth of 3.4 GHz, high porosity carbon was produced from rice husks by Wu et al. via KOH activation and one-step carbonization [6]. Almond shells were used by Fang et al. to produce porous carbon with an effective absorption bandwidth of 13.8 GHz and RL_{min} of -30 dB [7].

The composite materials that incorporate biomass carbon exhibit remarkable properties, especially when they are combined with other substances like ferrite, further enhancing their absorption capabilities [8-10]. In addition, the incorporation of a bio-based carbon component offers a sustainable and environmentally beneficial attribute, effectively resolving concerns related to the environment [11]. The application process of this composite material is facilitated by its lightweight nature. The results are encouraging, especially when considered in conjunction with the low-effort integration of Fe_3O_4 nanoparticles onto its surface using conventional methods. This composite makes use of both the biochar's porous structures and Fe_3O_4's magnetic properties. In their study, Zhao et al. conducted an experiment where they integrated Fe_3O_4 nanoparticles with highly porous carbon derived from walnut shells [12]. The resulting composite material exhibited an RL_{min} of -40.3 dB at a thickness of 2.0 mm, along with an effective absorption bandwidth spanning 6.6 GHz. Wang et al. successfully combined porous carbon from jute with Fe_3O_4 nanoparticles, resulting in an impressive RL_{min} of -39.5 dB at 2.0 mm and a wide effective absorption bandwidth of 4.0 GHz [13]. Currently, researchers have identified a constraint on the concurrent improvement of two factors: the intensity of absorption and the width of the effective absorption band.

Therefore, employing a two-step production procedure, the present study developed a composite material comprising Fe_3O_4 nanoparticles and porous carbon generated from rice husk. A comprehensive analysis was conducted on the absorption characteristics of the composite material within the frequency range of 2 to 18 GHz. The composite material exhibits distinct features that significantly boost its efficiency in absorbing microwaves, rendering it an especially attractive candidate for application in the electromagnetic realm.

2. Experiment

2.1. Material synthesis

Porous carbon (PC) material was synthesized from rice husks using a two-step carbonization process. The rice husks were first subjected to purification through a process of washing with deionized water, followed by drying at a temperature of 50°C. Subsequently, the husks were carbonized in a tube furnace under a nitrogen environment, at a rate of 5 °C/min, for a duration of 1 h, at a temperature of 400°C. A 150 mL solution of 5 mol/L KOH was used to immerse 5 g of carbonized rice husks for 24 h. Following a washing procedure using a HCl and water solution, the rice husks underwent vacuum drying at a temperature of 60°C. The carbonized rice husks underwent annealing at a temperature of 700°C in the presence of flowing nitrogen for a duration of 2 h, with a heating rate of 5°C per minute. The resulting samples were further neutralized to achieve a pH level using a 1 mol/L HCl solution and distilled water. The samples were then dried at a temperature of 60°C to obtain the porous carbon materials. Coprecipitation was used to make the Fe_3O_4/C composite material. 100 mL of DI water, 4 mmol of $FeCl_3$, and 2 mmol of $FeCl_2$ were mixed together to form a solution. Stirring at room temperature was carried out for 30 minutes, allowing the porous carbon to gradually add into the mixture. The observed mass fraction between Fe_3O_4 and Carbon is determined to be in a ratio of 2:1. The stirring process continued for an hour. Subsequently, 4 mL of NH_3 solution was added dropwise to the mixture. Mechanical stirring was maintained for 4 h at 60°C to facilitate the coprecipitation reaction. After several washes with water and ethanol, the powder was dried under vacuum at 60°C for 12 h.

2.2. Material characterization

The structural properties of the Fe_3O_4/C composite were investigated by X-ray diffraction (XRD) from 10^o to 70^o on a Bruker D5 with CuK1 radiation = 1.54056 Å. The morphological properties were characterized using scanning electron microscopy (SEM - S4800), and energy-dispersive X-ray spectroscopy (EDX). The magnetic measurements were conducted using a Lakeshore 7400 vibrating sample magnetometer (VSM). The measurement of the specific surface area and pore structures of composite materials was conducted by the process of nitrogen adsorption-desorption.

The experiment revealed that the Fe_3O_4/C material exhibited encouraging blending characteristics when combined with paraffin wax at a concentration of 30% by mass. Once the mixes were molded into a toroidal configuration, their internal diameter measured 3.04 mm, while the external diameter measured 7.00 mm. The microwave absorption properties were determined using the Keysight PNA-X N5242A vector network analyzer. The microwave absorption characteristics were calculated using the

transmission line method. The following equations provide a comprehensive comprehension of the reflection loss (RL) [14]:

$$RL(dB) = 20.\log\left|\frac{Z_{in}-1}{Z_{in}+1}\right| \quad (1)$$

$$Z_{in} = \sqrt{\frac{\mu_r}{\varepsilon_r}}\tanh\left(j\frac{2\pi fd}{c}\sqrt{\mu_r\varepsilon_r}\right) \quad (2)$$

The analysis of absorber input impedance (Z_{in}) involved the consideration of intricate relative permittivity (ε_r) and permeability (μ_r). Additional factors considered in this study were the thickness of the sample (d), the frequency of the incident light (f), and the velocity of light propagation in a vacuum (c).

3. Results and discussion

The porous carbon compounds that result from rice husks are shown as SEM images in Fig. 1a. The image demonstrates that the porous 3D carbon structures are formed from rice husks with numerous pores on the surface. The SEM images of the Fe_3O_4/C composite are shown in Fig. 1b. The results demonstrated the presence of Fe_3O_4 nanoparticles on the surfaces of carbon-based materials. Because of their porous structure, the Fe_3O_4 ferrite particles are rather evenly spread and have a tendency to adhere to surfaces. The diameter of Fe_3O_4 nanoparticles ranges from 5 to 10 nm.

In order to further examine the porous structure of the sample, the N_2 adsorption-desorption isotherms of both the carbon and Fe_3O_4/C samples were measured. The data presented in Fig. 1(c, d) demonstrates a notable trend in the adsorption capacity as a function of relative pressure. Specifically, it is observed that at low relative pressures, the adsorption capacity exhibits a rapid increase. This suggests that the adsorption process is highly efficient in this regime. Furthermore, the adsorbed N_2 molecules are found to occupy the micropores in the form of monolayers, indicating a single layer of molecules being adsorbed on the surface. The observed phenomenon of an evident hysteresis loop in the curve, in response to an elevated relative pressure, suggests the presence of mesoporous characteristics in carbon and Fe_3O_4/C materials. The porous carbon has an impressively high specific surface area of 48.8 m^2/g. This suggests that there is a great deal of surface area accessible for interactions. The material has small pores, with an average pore diameter of between 1.98 and 3.50 nm (Fig. 1e). Significant amounts of interacting surface are present on the Fe_3O_4/C material, as indicated by its high specific surface area of 220.6 m^2/g. The material's typical pore diameters are highly concentrated at 1.10 and 1.36 nm (Fig. 1f), indicating the presence of clearly defined pore structures.

Because of its surface interactions and pore accessibility, the material has a wide range of possible uses. The specific surface area of the Fe_3O_4/C material is about 4.5 times higher than that of pure carbon, making it a distinguishing feature. It has been discovered that surface modification aids in the formation of pore structure. Increasing the sample's specific surface area increases its ability to absorb electromagnetic waves and lengthens the path along which they propagate.

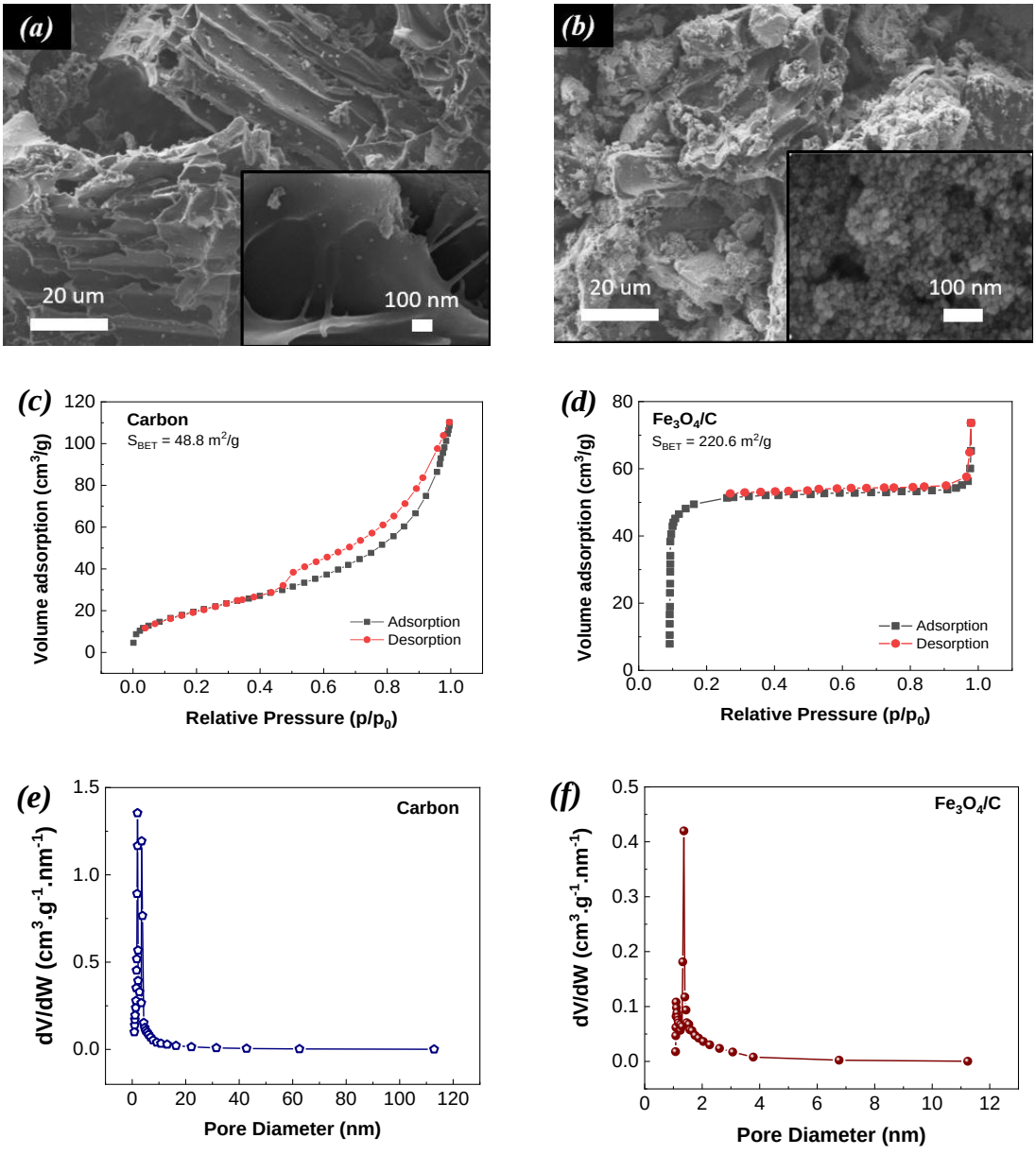

Fig. 1. SEM images (a, b), N_2 adsorption-desorption isotherms (c, d), and pore diameter distribution curves (e, f) of PC and Fe_3O_4/C.

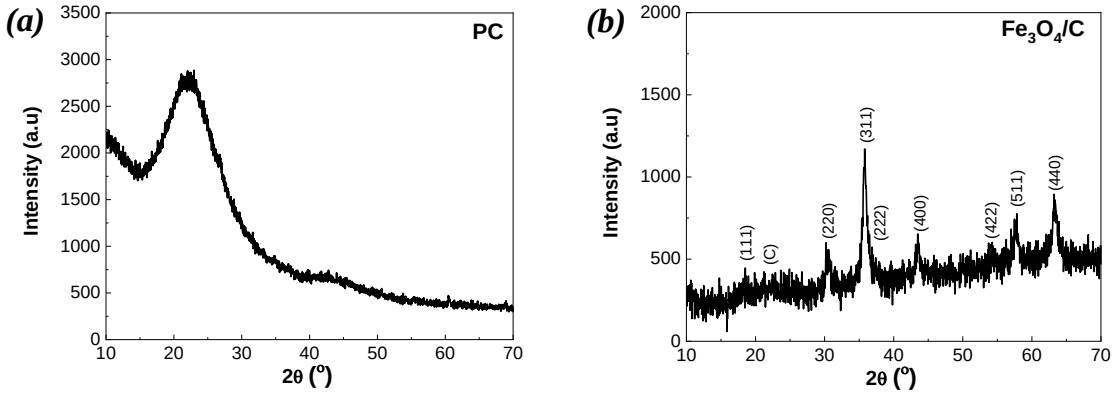

Fig. 2. XRD patterns of PC (a) and Fe_3O_4/C (b).

X-ray diffraction (XRD) investigation was performed in order to determine the carbon phase depicted in Fig. 2a. The diffraction peaks observed at approximately 22° and 43° can be attributed to the (002) and (100) crystallographic planes of graphite carbon in the sample. The presence of these wide diffraction peaks suggests a low degree of graphitization in the PC material, indicating that the carbon structure is amorphous [6]. Fig. 2b shows the XRD patterns of an Fe_3O_4/C composite. The diffraction peak corresponding to C in the Fe_3O_4/C sample exhibits a relatively low intensity. This can be attributed to the extensive presence of Fe_3O_4 nanoparticles, which effectively cover the surface of the porous carbon material. The (111), (220), (311), (222), (400), (422), (511), and (440) crystal planes of the face-centered cubic trevorite structure are assigned the diffraction peaks of 18.5°, 30.2°, 36.8°, 36.9°, 43.5°, 54.1°, 57.8°, and 63.2°, respectively [12]. The Fe_3O_4/C composite's EDX spectrum is seen in Fig. 3. Carbon-Fe_3O_4 nanocomposites were successfully synthesized, as evidenced by the examination of this picture, which also reveals the presence of Fe, O, and C inside the sample. Within the composite material, a minor percentage of silicon is obtained from the organic source of rice husk. This content facilitates the attachment of Fe_3O_4 nanoparticles onto the carbon layer's surface while also enhancing the efficiency of electromagnetic wave absorption through dielectric loss.

The magnetic properties of both Fe_3O_4 and Fe_3O_4/C composite materials were examined using a vibrating sample magnetometer. As illustrated in Fig. 4, the hysteresis loops of Fe_3O_4 and Fe_3O_4/C composites exhibit characteristic S-shaped curves, indicating the presence of superparamagnetic properties in the samples [8]. The coercive force (Hc) values of the Fe_3O_4 and Fe_3O_4/C samples are 3 and 9 Oe, respectively. The remanence (Mr) of the aforementioned two samples is approximately 0.7 emu/g. Furthermore, the magnetic saturation (Ms) of Fe_3O_4 was observed to be 61.5 emu/g, whereas Fe_3O_4/C exhibited a magnetic saturation of 38.9 emu/g. The decrease in the Ms value primarily

arises from the incorporation of a non-magnetic Carbon component into the composite material. The observed ratio between the magnetic saturation value of Fe_3O_4/C and Fe_3O_4 is in agreement with both the initial material ratio and the results obtained from the EDX analysis of the composite.

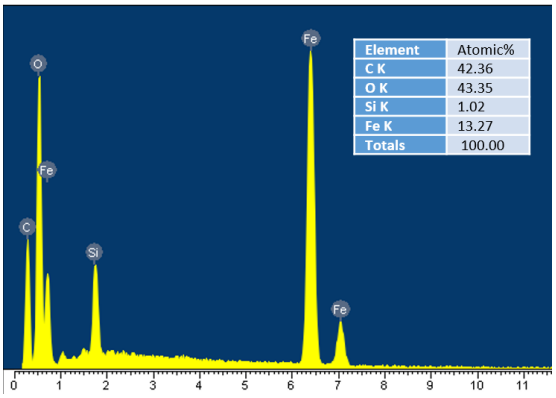

Fig. 3. EDX spectrum of Fe_3O_4/C composite.

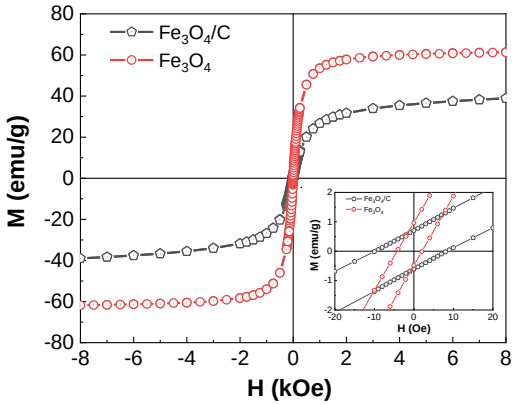

Fig. 4. Magnetic hysteresis loop of Fe_3O_4/C composite at room temperature.

Figure 5 illustrates the correlation between the frequency-dependent characteristics of the real and imaginary constituents of complex permittivity and complex permeability. As the frequency increases, there is a decrease observed in both the real and imaginary components of permittivity. The electronic polarisation, interfacial polarisation, and ionic polarisation contributions to the complex permittivity are highly influenced by the structural features and surface morphology [15]. Charge transport and interfacial polarisation can be improved by a porous structure's high surface area. The sustained wave propagation through the three-dimensional structure of the material system is indicated by a slight frequency-dependent decrease in the real component of complex permittivity. As the frequency increases, the imaginary part of the complex permittivity reduces significantly, suggesting that the dielectric absorption process relies mostly on natural polarisation. Within the frequency range spanning from 2 to 18 GHz, there is a discernible and consistent decrease observed in the real component of the complex permeability. Conversely, the imaginary component exhibits very minor variations. The alterations in the magnetic characteristics occurring at the interface between the Fe_3O_4/C layers, specifically in the presence of surface defects, exert a significant influence on the distinctions observed in the imaginary component of the permeability.

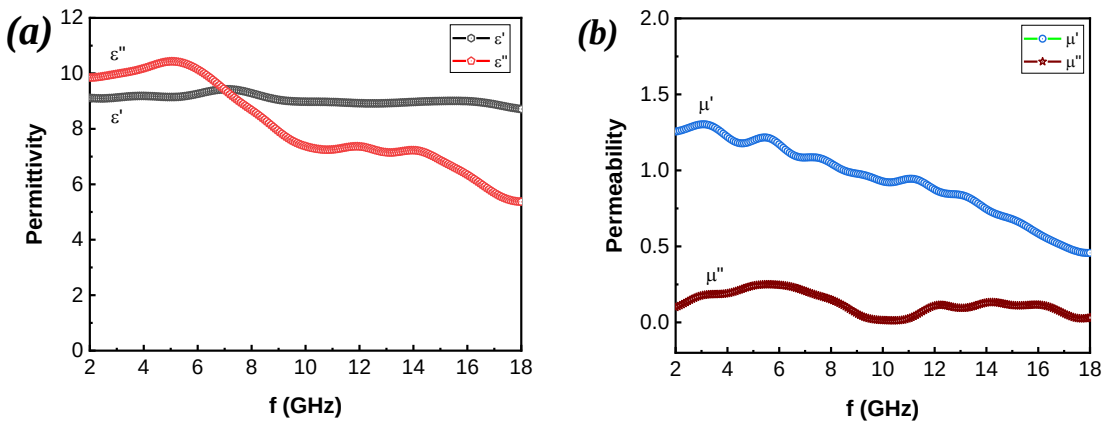

Fig. 5. The complex permittivity (a) and complex permeability (b) of Fe_3O_4/C composite.

Based on the Debye theory, the relationship between ε' and ε'' is demonstrated by the Cole-Cole equation (Eq. 3). A Cole-Cole semicircle is evidence of a Debye relaxation process, as proposed by Debye theory [9].

$$\left(\varepsilon' - \frac{\varepsilon_s + \varepsilon_\infty}{2}\right)^2 + \left(\varepsilon''\right)^2 = \left(\frac{\varepsilon_s - \varepsilon_\infty}{2}\right)^2 \quad (3)$$

where ε_s, ε_∞ are the static permittivity and the high-frequency limit relative permittivity, respectively.

The presence of a large number of discrete semicircles, as seen in Fig. 6a, is suggestive of a sophisticated relaxation event involving a number of different dielectric components in the composite material. The presence of dielectric loss-increasing processes, such as defect polarisation and interfacial polarisation, is demonstrated by distorted Cole-Cole semicircles [8]. If there is an external electromagnetic field present, then there is a possibility that additional polarisation centers will arise at the heterogeneous interfaces of Fe_3O_4/C. The polarisation of interfaces is improved as a result of this impact, as are the relaxation processes that take place at those interfaces.

The magnetic loss caused by eddy currents can be approximated using the coefficient C_0, with the formula $C_0 = \mu''/(\mu'^2.f)$, where f is the frequency [10]. Eddy current loss dominates magnetic loss if C_0 remains constant. It is important to note that low-frequency variations are caused by natural resonance, whereas high-frequency variations are caused by exchange resonance [13]. As can be seen in Fig. 6b, the C_0 value exhibits rather substantial fluctuations, trending downwards in the low frequency zone and upwards in the high frequency region. It demonstrates that natural resonance, specifically exchange resonance, is the primary mechanism of loss. Furthermore, in the

frequency range from 9 to 11 GHz, the absorption process, which is the eddy current loss, corresponds to a slight change in the C_0 value.

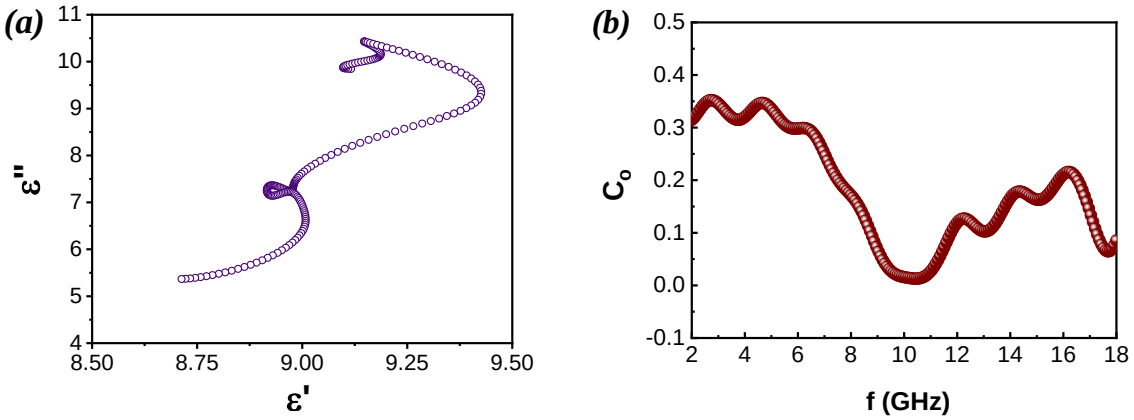

Fig. 6. The typical Cole-semicircle curve (a) and C_0 - f values (b) of Fe_3O_4/C composite.

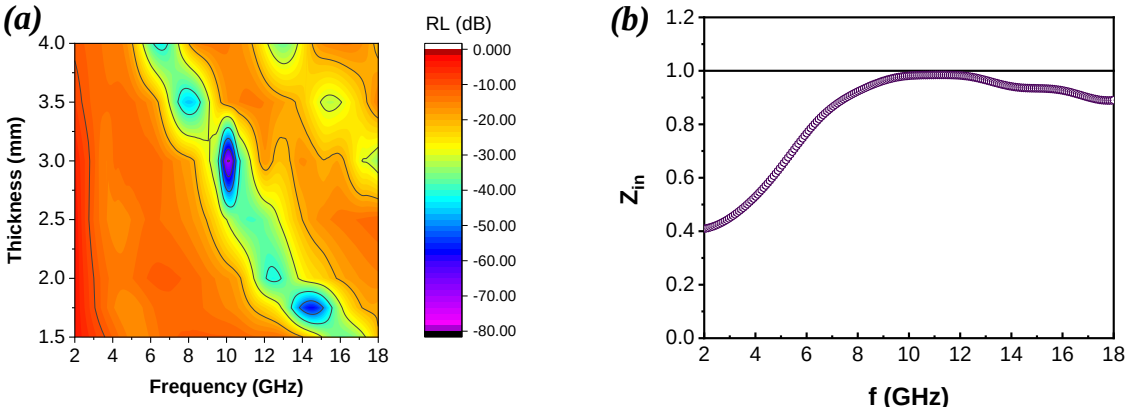

Fig. 7. The reflection loss (a) and Z_{in} (b) of Fe_3O_4/C sample.

RL measurements can be taken on objects with a thickness of 1.5 - 4.0 mm and a frequency of 2 - 18 GHz. The variety of RL values for Fe_3O_4/C composites is shown on a contour plot RL graph in Fig. 7a. The material is ideal for microwave absorbing engineering applications since it absorbs more than 90% of incident EM. When the absorber thickness is changed from 1.5 to 4.0 mm, most samples achieve a minimum RL of less than -10 dB (90% decrease) across a wide range of electromagnetic frequencies (3.6 to 18 GHz). The effective absorption bandwidth (EAB) is 14.4 GHz (from 3.6 to 18 GHz) at a thickness of only 1.5 mm. Specifically, when the thickness is 4.0 mm, the EAB spans the entire frequency range from 2 to 18 GHz. As the thickness increases, the lowest frequency at which the reflection loss reaches its minimum value (RL_{min}) shifts downward. With a thickness of just 3.0 mm, the Fe_3O_4/C composite displays an

impressive reflection loss of -70.8 dB at a frequency of 10.1 GHz. Furthermore, the frequency bands where over 99% of microwave absorption happens at this thickness are between 8.3 and 11.7 GHz, which is 3.4 GHz.

Figure 7b depicts the impedance values (Z_{in}) of the Fe_3O_4/C composite when the thickness is 3.0 mm. The impedance values of Fe_3O_4/C demonstrate a close approach to 1 in the frequency range of 9.8 to 12.2 GHz, suggesting an ideal impedance match within this particular band. The Fe_3O_4/C material exhibits a structure that is both hollow and porous, facilitating the increased penetration of incident electromagnetic waves. As a result, there is an improvement in impedance matching [13]. It is noteworthy to notice that there is a strong alignment between the frequency range at which effective impedance matching takes place and the frequency range of EAB for Fe_3O_4/C.

Table 1 compares ferrite-biomass carbon composites. This research found that Fe_3O_4/C composite absorb microwaves significantly. Thin thickness, large absorption bandwidth, and considerable reflection loss are these features.

Table 1. Comparison of the microwave absorption properties with other absorbers

Absorber	**RL_{min} (dB)**	**EAB (GHz)**	**d (mm)**	**Ref.**
C (rice husks)	-47.5	3.4	2.8	[6]
C (almond shells)	-30.0	13.8	-	[7]
Fe_3O_4-C (walnut shells)	-40.3	6.6	2.0	[12]
Fe_3O_4-C (jute)	-39.5	4.0	2.0	[13]
FeO_X-C (coconut shells)	-26.5	2.5	6.5	[16]
Fe/Fe_3O_4/C (agaric)	-30.4	2.45	2.0	[19]
$NiFe_2O_4$-C (pomelo peels)	-50.8	2.5	4.9	[18]
Fe_3O_4/C (rice husk)	-57.6 -70.8	14.9 11.4	1.75 3.0	This work

The electromagnetic wave absorption properties of Fe_3O_4/C materials are determined by their microstructure. The phenomenon of dielectric and magnetic loss in nature has been observed to play a role in enhancing impedance matching and electromagnetic wave absorption [9]. Furthermore, the three-dimensional structure of the carbon material obtained from rice husks enhances the dispersion of electromagnetic microwaves within its tubes on multiple occasions. Additionally, it is imperative to recognize that Fe_3O_4/C displays a higher surface area when compared to pure porous carbon [16]. This specific attribute potentially contributes to its increased ability to efficiently absorb electromagnetic radiation. The presence of dipole polarization in porous carbon material is attributed to the presence of functional groups and surface defects, as mentioned in reference [17]. The spreading of Fe_3O_4 nanoparticles on the

surface of the porous carbon layers results in an enhancement of their microwave absorption characteristic. Enhancements in the microwave absorption properties of Fe_3O_4/C could be potentially attained through the investigation of many aspects, including polarisation, electron hopping, and the interface between Fe_3O_4 and C materials [8]. The process of absorbing incoming wave energy and converting it into thermal energy through microcurrents can be primarily attributed to the alternating rotation of magnetic domains and the exchange of magnetic energy between Fe_3O_4 nanoparticles [18].

4. Conclusion

In conclusion, the synthesis of well-dispersed Fe_3O_4 nanoparticles decorated on the porous carbon surface can be achieved through the combined utilization of the pyrolysis technique and the annealing process. Fe_3O_4/C composite, which possesses specific structural characteristics, exhibits substantially enhanced microwave absorption capabilities. This improvement can be attributable to the combination of superior attenuation and impedance matching. The interaction between the number of Fe_3O_4 nanoparticles, the material's conductive loss, and the material's polarization relaxation results in a microwave absorption performance that can be tuned according to specific requirements. At a filler loading of 30%, the composite obtains a minimum reflection loss (RL_{min}) of -70.8 dB with a thickness of 3.0 mm, as well as an effective absorption bandwidth (EAB) of 14.4 GHz with a thickness of just 1.5 mm. With its low manufacturing cost and ease of preparation, carbon extracted from rice husks provides the path for the development of magnetic carbon-based composites with superior wave absorption properties. The Fe_3O_4/C composite suggests a new blueprint for the design of magnetic biomass carbon composite absorbers.

Acknowledgement

This research is funded by Le Quy Don Technical University Research Fund under grant number 2023.QHT.02.

References

[1] P. T. Tho, C. T. A. Xuan, N. Tran, N. Q. Tuan, W. H. Jeong, S. W. Kim, T. Q. Dat, V. D. Nguyen, T. N. Bach, T. D. Thanh, D. T. Khan, and B.W. Lee, "Ultra-wide effective absorption bandwidth of Cu, Co, and Ti co-doped $SrFe_{12}O_{19}$ hexaferrite," *Ceram. Int.*, Vol. 48, No. 19, pp. 27409-27419, 2022. DOI: 10.1016/j.ceramint.2022.05.389

[2] H. Pang, Y. Duan, L. Huang, L. Song, J. Liu, T. Zhang, X. Yang, J. Liu, X. Ma, J. Di, and X. Liu, "Research advances in composition, structure and mechanisms of microwave absorbing materials," *Compos. B. Eng.*, Vol. 224, 2021, 109173. DOI: 10.1016/j.compositesb.2021.109173

[3] A. Houbi, Z. A. Aldashevich, Y. Atassi, Z. B. Telmanovna, M. Saule, and K. Kubanych, "Microwave absorbing properties of ferrites and their composites: A review," *J. Magn. Magn. Mater.*, Vol. 529, 2021, 167839. DOI: 10.1016/j.jmmm.2021.167839

[4] R. Qiang, S. Feng, Y. Chen, Q. Ma, and B. Chen, "Recent progress in biomass-derived carbonaceous composites for enhanced microwave absorption," *J. Colloid Interface Sci.*, Vol. 606 (1), pp. 406-423, 2022. DOI: 10.1016/j.jcis.2021.07.144

[5] H. Guan, Q. Wang, X. Wu, J. Pang, Z. Jiang, G. Chen, C. Dong, L. Wang, and C. Gong, "Biomass derived porous carbon (BPC) and their composites as lightweight and efficient microwave absorption materials," *Compos. B. Eng.*, Vol. 207, 2021, 108562. DOI: 10.1016/j.compositesb.2020.108562

[6] Z. Wu, Z. Meng, C. Yao, Y. Deang, G. Zhang, and Y. Wang, "Rice husk derived hierarchical porous carbon with lightweight and efficient microwave absorption," *Mater. Chem. Phys.*, Vol. 275, 2022, 125246. DOI: 10.1016/j.matchemphys.2021.125246

[7] X. Fang, W. Li, X. Chen, Z. Wu, Z. Zhang, and Y. Zou, "Controlling the microstructure of biomass-derived porous carbon to assemble structural absorber for broadening bandwidth," *Carbon*, Vol. 198, pp. 70-79, 2022. DOI: 10.1016/j.carbon.2022.06.074

[8] T. Q. Dat, N. T. Ha, and D. Q. Hung, "Reduced graphene oxide-$Cu_{0.5}Ni_{0.5}Fe_2O_4$-Polyaniline nanocomposite: Preparation, characterization and microwave absorption properties," *J. Electron. Mater.*, Vol. 46, pp. 3707-3713, 2017. DOI: 10.1007/s11664-017-5386-z

[9] N. V. Tung, T. Q. Dat, N. T. Ha, N. T. Nam, and D. Q. Hung, "Synthesis of reduced graphene oxide - $Mn_{0.8}Zn_{0.2}Fe_2O_4$ - porous polyaniline nanocomposite materials for effective microwave absorption in X-band," *Journal of Science and Techique*, Vol. 15 (5), pp. 13-23, 2020. DOI: 10.56651/lqdtu.jst.v15.n05.81

[10] T. Q. Dat, N. T. Ha, N. V. Tung, and P. V. Thin, "Microwave absorption performances of copper/nickel ferrite@fiber polyaniline," *Journal of Science and Techique*, Vol. 16 No. 02, pp. 5-13, 2021. DOI: 10.56651/lqdtu.jst.v16.n02.262

[11] R. Peymanfar and A. Ali Mirkhan, "Biomass-derived materials: Promising, affordable, capable, simple, and lightweight microwave absorbing structures," *J. Chem. Eng.*, Vol. 446 (1), 2022, 136903. DOI: 10.1016/j.cej.2022.136903

[12] H. Zhao, Y. Cheng, H. Lv, G. Ji, and Y. Du, "A novel hierarchically porous magnetic carbon derived from biomass for strong lightweight microwave absorption," *Carbon*, Vol. 142, pp. 245-253, 2019. DOI: 10.1016/j.carbon.2018.10.027

[13] L. Wang, H. Guan, J. Hu, Q. Huang, C. Dong, W. Qian, and Y. Wang, "Jute-based porous biomass carbon composited by Fe_3O_4 nanoparticles as an excellent microwave absorber," *J. Alloys Compd.*, Vol. 803, pp. 1119-1126, 2019. DOI: 10.1016/j.jallcom.2019.06.351

[14] C. T. A. Xuan, P. T. Tho, T.Q. Dat, N. V. Khien, T. N. Bach, N. T. M. Hong, T. A. Ho, D. T. Khan, H. N. Toan, and N. Tran, "Development of high-efficiency microwave absorption properties of $La_{1.5}Sr_{0.5}NiO_4$ and $SrFe_{12}O_{19}$-based materials composites," *Surf. Interfaces.*, Vol. 39, 2023, 102890. DOI: 10.1016/j.surfin.2023.102890

[15] J. Wang, M. Zhou, Z. Xie, X. Hao, S. Tang, J. Wang, Z. Zou, and G. Ji, "Enhanced interfacial polarization of biomass-derived porous carbon with a low radar cross-section," *J. Colloid Interface Sci.*, Vol. 612, pp. 146-155, 2022. DOI: 10.1016/j.jcis.2021.12.162

[16] L. Wang, H. Guan, S. Su, J. Hu, and Y. Wang, "Magnetic FeO_X/biomass carbon composites with broadband microwave absorption properties," *J. Alloys Compd.*, Vol. 903, 2022, 163894. DOI: 10.1016/j.jallcom.2022.163894

[17] X. Lu, X. Li, W. Zhu, and H. Xu, "Construction of embedded heterostructures in biomass-derived carbon frameworks for enhancing electromagnetic wave absorption," *Carbon*, Vol. 191, pp. 600-609, 2022. DOI: 10.1016/j.carbon.2022.01.050

[18] Y. Wang, X. Gao, H. Zhou, X. Wu, W. Zhang, Q. Wang, and C. Luo, "Fabrication of biomass-derived carbon decorated with $NiFe_2O_4$ particles for broadband and strong microwave absorption," *Powder Technol.*, Vol. 345, pp. 370-378, 2019. DOI: 10.1016/j.powtec.2019.01.025

[19] J. Su, R. Yang, P. Zhang, B. Wang, H. Zhao, W. Zhang, W. Wang, and C. Wang, "Fe/Fe_3O_4/biomass carbon derived from agaric to achieve high-performance microwave absorption," *Diam. Relat. Mater.*, Vol. 129, 2022, 109386. DOI: 10.1016/j.diamond.2022.109386

TỔNG HỢP HẠT NANO Fe_3O_4 TRÊN CACBON XỐP THU ĐƯỢC TỪ VỎ TRẤU ĐỂ TĂNG CƯỜNG HẤP THỤ VI SÓNG

Phạm Văn Thìn[a], Lê Đình Vị[a], Nguyễn Văn Tuấn[a], Nguyễn Trần Hà[a], Nguyễn Vũ Tùng[a], Nguyễn Thị Thanh[a], Trần Quang Đạt[a]

[a]*Khoa Hóa - Lý kỹ thuật, Trường Đại học Kỹ thuật Lê Quý Đôn*

Tóm tắt: Trong nghiên cứu này, một quy trình hiệu năng đã được sử dụng để tổng hợp cacbon xốp được phủ bởi các hạt nano Fe_3O_4 có nguồn gốc từ phế thải vỏ trấu (Fe_3O_4/C). Vật liệu composite được tạo ra bằng phương pháp nhiệt phân và đồng kết tủa. Các hạt nano Fe_3O_4 được phân tán đều trên bề mặt cấu trúc ba chiều của cacbon xốp. Khung cacbon xốp được graphit hóa cao tạo ra các rãnh cho sóng điện từ lan truyền lâu hơn và làm tăng khả năng mất độ dẫn điện. Với cấu trúc độc đáo và hiệu ứng suy hao lớn, kết hợp trở kháng tốt, vật liệu Fe_3O_4/C hấp thụ vi sóng tốt hơn nhiều so với cacbon xốp. Hầu hết các mẫu có suy hao phản xạ (RL) nhỏ hơn -10 dB (giảm 90%) trên dải tần số điện từ rộng (3,6 - 18 GHz) khi độ dày của mẫu hấp thụ thay đổi từ 1,5 - 4,0 mm. Với độ dày 3,0 mm, RL tốt nhất là -70,8 dB và với độ dày của mẫu là 1,5 mm, băng thông hấp thụ hiệu quả là 14,4 GHz. Theo kết quả của nghiên cứu này, việc sử dụng vật liệu Fe_3O_4/C cho các ứng dụng hấp thụ sóng điện từ có nhiều triển vọng do chi phí thấp và lợi ích mở rộng của quy trình điều chế cũng như hiệu suất hấp thụ của chúng.

***Từ khóa**: Fe_3O_4; ferit; vật liệu sinh học; vỏ trấu; vật liệu hấp thụ.*

Received: 14/08/2023; Revised: 14/09/2023; Accepted for publication: 17/11/2023

❑